Ground-State Chemical Reactivity under Vibrational Coupling to the Vacuum Electromagnetic Field

Anoop Thomas, Jino George, Atef Shalabney, Marian Dryzhakov, Sreejith Jayasree Varma, Joseph Moran, Thibault Chervy, Xiaolan Zhong, Eloïse Devaux, Cyriaque Genet, et al.

Kinetics Hot Paper

International Edition: DOI: 10.1002/anie.201605504
German Edition: DOI: 10.1002/ange.201605504

Ground-State Chemical Reactivity under Vibrational Coupling to the Vacuum Electromagnetic Field

*Anoop Thomas[+], Jino George[+], Atef Shalabney, Marian Dryzhakov, Sreejith J. Varma, Joseph Moran, Thibault Chervy, Xiaolan Zhong, Eloïse Devaux, Cyriaque Genet, James A. Hutchison, and Thomas W. Ebbesen**

Abstract: *The ground-state deprotection of a simple alkynylsilane is studied under vibrational strong coupling to the zero-point fluctuations, or vacuum electromagnetic field, of a resonant IR microfluidic cavity. The reaction rate decreased by a factor of up to 5.5 when the Si–C vibrational stretching modes of the reactant were strongly coupled. The relative change in the reaction rate under strong coupling depends on the Rabi splitting energy. Product analysis by GC-MS confirmed the kinetic results. Temperature dependence shows that the activation enthalpy and entropy change significantly, suggesting that the transition state is modified from an associative to a dissociative type. These findings show that vibrational strong coupling provides a powerful approach for modifying and controlling chemical landscapes and for understanding reaction mechanisms.*

The direct excitation of a given vibrational mode to influence chemical reactivity has long been a topic of interest as it could lead to site-selective chemical reactions and enable the elucidation of reaction mechanisms. Pimentel and co-workers demonstrated in the 1980s that they could use infrared lasers to influence the outcome of simple reactions, but this could only be done at cryogenic temperatures as competing thermal effects and relaxation processes had to be minimized.[1,2]

An alternative approach to modifying the chemical landscape is to hybridize a molecular transition with the zero-point fluctuations of the optical mode of a cavity in which the molecules are placed, as we demonstrated for the first time in 2011.[3] This involved the coupling of the electronic transition of merocyanine and splitting the first excited state into two hybrid light–matter states, which significantly slowed the photochemical reactivity and increased the yield. As we concluded,[3] a specific vibrational transition could in principle also be coupled, which should in turn modify the reactivity of a given bond. To confirm this prediction, we and other groups have been studying vibrational strong coupling to infrared cavities[4–8] and shown that vibrational transitions of both solids and liquids can be split as schematically illustrated in Figure 1 a. This in turn should affect the Morse potential and, more generally, the reactivity landscape in the ground state.

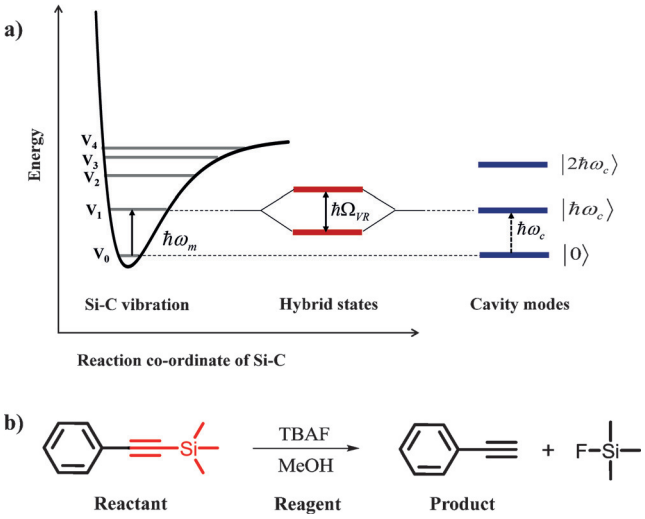

Figure 1. a) The light–matter strong coupling between the Si–C stretching vibrational transition and a cavity mode that results in the Rabi splitting. b) The silane deprotection reaction of 1-phenyl-2-trimethylsilylacetylene used in the present study.

After all, it is well known that non-adiabatic processes play a critical role in chemical reactivity and that at conical intersections, for instance, the Born–Oppenheimer approximation breaks down owing to strong interactions between the electronic and vibrational manifolds.[9]

To investigate whether ground-state chemical reactivity can indeed be influenced by vibrational strong coupling, the deprotection reaction of an alkynylsilane, 1-phenyl-2-trimethylsilylacetylene (PTA), with tetra-*n*-butylammonium fluoride (TBAF) was chosen as a prototypical reaction (Figure 1 b).[10] This simple system presents several practical advantages for the demonstration of such an effect. PTA is a pure liquid and can therefore be injected directly into a microfluidic Fabry–Perot cavity. The reactant has relatively few well-defined strongly absorbing vibrational modes. Fur-

[*] Dr. A. Thomas,[+] Dr. J. George,[+] Dr. M. Dryzhakov, S. J. Varma, Dr. J. Moran, T. Chervy, Dr. X. Zhong, Dr. E. Devaux, Dr. C. Genet, Dr. J. A. Hutchison, Prof. Dr. T. W. Ebbesen
University of Strasbourg, CNRS, ISIS & icFRC
8 allée G. Monge, 67000 Strasbourg (France)
E-mail: ebbesen@unistra.fr
Dr. A. Shalabney
Braude College
Snunit St 51, Karmiel 2161002 (Israel)
[+] These authors contributed equally to this work.

Supporting information for this article can be found under: http://dx.doi.org/10.1002/anie.201605504.

thermore, the deprotection reaction occurs by pseudo-first-order kinetics on a timescale of minutes so that it can be monitored by FTIR spectroscopy at different time intervals.

The cavity consists of two parallel mirrors separated by a distance on the order of 6 μm that can be tuned precisely to be in resonance with the vibrational transitions of the reactant. The IR transmission of the cavity and reactant system is shown for a broad spectral range in Figure 2a. Figure 2b focuses on a smaller spectral window to show how the transmission spectrum of the cavity (red curve) is modified by the vibrational absorption spectrum of PTA (blue curve). The cavity is tuned so that it is resonant with the stretching transitions of the C–Si bond around 860 cm^{-1}, a double peak corresponding to the C≡C–Si and –Si(–Me)$_3$ modes.

Such a cavity of length L has a series of resonances (Figure 2a), which are multiples of the fundamental cavity mode and depend on the refractive index n of the medium inside the cavity such that the wavelength λ is equal to $2nL/m$, where m (mode order) is an integer. Correspondingly, in wavenumber units, $\overline{\nu}(cm^{-1}) = \frac{10^4}{\lambda} = \frac{10^4 m}{2nL}$, with L and λ in μm. As a consequence, another cavity mode falls exactly on the –C≡C– stretching transition at 2160 cm^{-1}. If the product and the reactants have even slightly different refractive indices, then the positions of the cavity resonances that lie far from any vibrational absorption peak can be conveniently monitored to follow the chemical reaction as we shall see below.

Vibrational strong coupling, VSC, is achieved by placing a molecular material in the confined field of an optical cavity mode that is resonant with a vibrational transition. This splits the vibrational levels into two new hybrid states, which are separated by the Rabi splitting $\hbar\Omega_{VR}$ (Figure 1a). The magnitude of the Rabi splitting reflects the strength of the interaction, and it is proportional to the square root of the absorbance of the peak and therefore to the concentration (Figure 3a, inset) and the molar extinction coefficient. VSC occurs even in the dark as it is

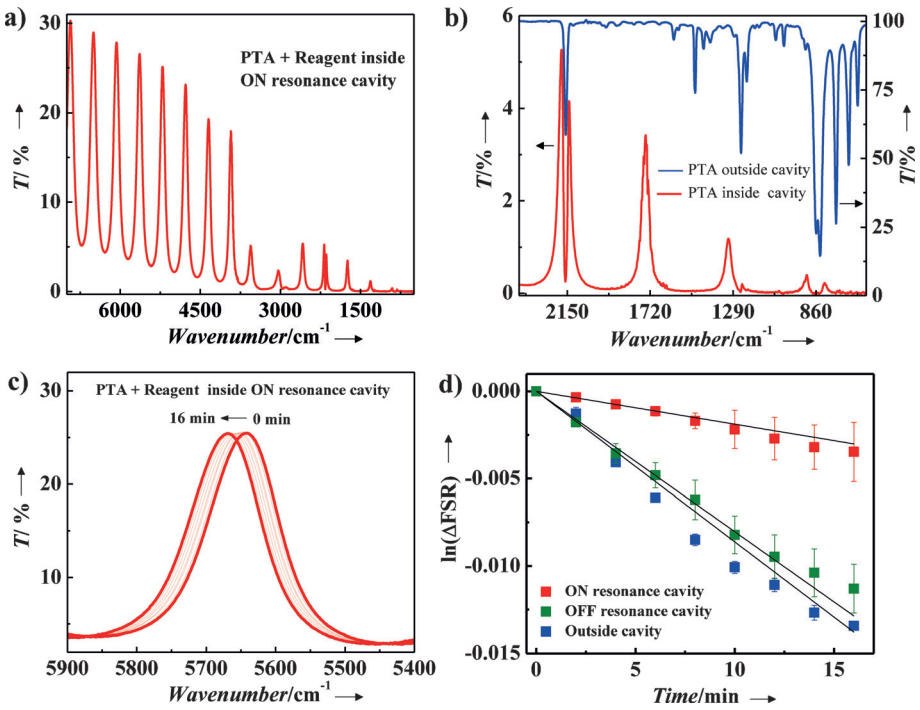

Figure 2. a) IR transmission spectrum of the ON resonance cavity from 7000 to 500 cm^{-1} immediately after injection of the reaction mixture (PTA+reagent). b) IR transmission spectrum of PTA inside (red trace) and outside (blue trace) the ON resonance cavity. c) Temporal shift of the higher-order cavity modes of the ON resonance cavity during the reaction (0 to 16 min). d) Kinetics of the reactions in an ON resonance cavity (red squares), outside the cavity (blue squares), and in an OFF resonance cavity (green squares) as extracted from the temporal shifts in the higher-order cavity modes. All measurements were carried out at [PTA] = 2.53 M. See the Experimental Section for details.

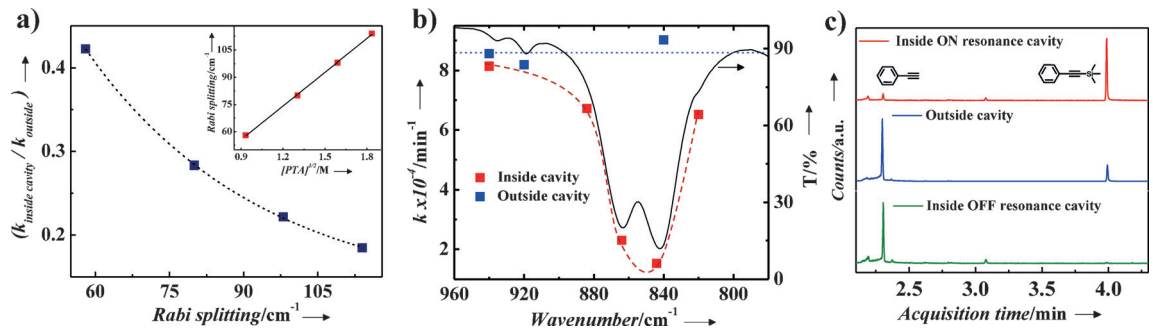

Figure 3. a) The decrease in the ratio of the reaction rates under VSC and outside the cavity as a function of the Rabi splitting energy. The inset shows the linear dependence of the Rabi splitting on the square root of [PTA]. b) The reaction rate as a function of the cavity tuning for reactions inside (red squares) and outside (blue squares) the cavity. The black solid line shows the double-peaked IR absorption spectrum associated with the Si–C modes of PTA. The dotted lines are guides to the eye. c) GC-MS chromatograms of silane deprotection reactions carried out inside the ON resonance cavity (red trace), in the OFF resonance cavity (green trace), and outside the cavity (blue trace). (The GC-MS data shown here correspond to experiments carried out at higher [PTA] (3.37 M, $\hbar\Omega_{VR}$ = 114 cm^{-1}), see the Experimental Section for details.)

a result of interactions between the zero-point energies of the optical and vibrational modes.[11] To ensure true VSC, it is important to confirm that the Rabi splitting is larger than the width of the vibrational and cavity resonances. Figure 2b shows the spectral splitting of the C–Si stretching transition with a Rabi splitting of 98 cm^{-1} (for [PTA] = 2.53 M), which is larger than the FWHM of both the vibrational transition of Si–C (39 cm^{-1}) as well as the respective cavity resonance (30 cm^{-1}; see the Supporting Information, Figure S1a). In contrast, the −C≡C− vibrational mode at 2160 cm^{-1} interacts with another cavity resonance but it does not meet this criterion for strong coupling.

The reaction was initiated by mixing PTA with TBAF in methanol and then injecting the mixture into an IR cavity that was either tuned to (ON resonance) or detuned from (OFF resonance) the C–Si stretching mode. The detuned case serves as a control experiment for the kinetics in the absence of VSC. An additional control experiment was carried out "outside" the cavity with both mirrors replaced by dielectric windows. The evolution of the system was followed by FTIR spectroscopy. As indicated above, as the reactant and products in this reaction have slightly different refractive indices, the shifts in the cavity resonances far from any vibrational absorption reflect the progress of the reaction as shown in Figure 2c. A ln plot of this shift versus time gives a straight line for both the tuned and detuned cavity but the rate constants are very different. Under VSC, the reaction rate constant decreased by a factor of 4.5 for [PTA] = 2.53 M (Figure 2d). The reaction rate was also studied as a function of the Rabi splitting energy (see below). It was confirmed that the detuned cavity gave roughly the same rate as a reaction outside the cavity (Figure 2d). The small differences are due to experimental errors. It is also important to note that the cavity mirrors were insulated with 100 nm glass to avoid any influence of the metal surfaces.

If the Rabi splitting varied during the reaction, one would not expect the linear plots of Figure 2d under VSC. However, unlike in our earlier study on the formation of merocyanine under electronic strong coupling,[3] here, the Rabi splitting hardly changes during the reaction because there are also Si–C modes present in the product (see Figure S1b). Hence the observed linearity probably implies that both the reactants and products are shaping the chemical landscape connecting them and strongly affect the transition state as shown below.

The dependence of the change in the reaction rate on the Rabi splitting was explored by varying [PTA]. As shown in the inset in Figure 3a, the Rabi splitting energy depends on the square root of the PTA concentration as expected. The Rabi splitting energy was varied from 58 cm^{-1} to 114 cm^{-1} by changing [PTA] from 0.87 M to 3.37 M, and the reaction rate was monitored under VSC and outside the cavity. Interestingly, the ratio of the reaction rate under VSC to the rate outside the cavity decreased with the Rabi splitting as shown in Figure 3a. In other words, the retardation of the reaction under VSC increases with the Rabi splitting. The reaction does not have a linear dependence on the Rabi splitting, which reflects the complex effect of VSC on the chemical landscape (see below). In Figure 3b, the reaction rate is plotted as a function of cavity tuning relative to the C–Si band (black curve) both for the mirrored cavity (red squares) and outside the cavity (blue squares) with different spacings between the dielectric windows (which give rise to a weak spectral response defining the position of the blue squares). The largest effect is clearly seen at resonance under VSC. The change in reactivity was also monitored qualitatively by GC-MS. As shown in Figure 3c, the product/reactant peak ratios were totally different when the reaction was stopped after 20 min, and the reaction mixture injected into the GC-MS column, providing absolute proof that the spectrally observed change in the reaction rate is indeed due to changes in the chemical reactivity. The product distributions for the reactions outside the cavity and in the detuned case were similar (the small variation in the reactant peak is within the experimental error of the present qualitative measurement) whereas product formation was clearly retarded in the resonant cavity.

To understand the changes in the chemical landscape induced by VSC, the reaction rate was also measured as a function of temperature to extract the thermodynamic parameters associated with the transition state (Figure 4) using the transition-state Eyring equation:

$$k = \frac{k_B T}{h} \exp\left(-\frac{\Delta H^{\ddagger}}{RT} + \frac{\Delta S^{\ddagger}}{R}\right) \quad (1)$$

The enthalpy $\Delta H^{\ddagger}$ and entropy $\Delta S^{\ddagger}$ of activation were extracted by plotting $\ln(k/T)$ as a function of $1/T$ (Figure 4) for [PTA] = 2.53 M and a Rabi splitting energy of 98 cm^{-1}. $\Delta H^{\ddagger}$ increased from 39 to 96 kJ mol^{-1} under VSC while $\Delta S^{\ddagger}$ increased from −171 to 7.4 J K^{-1} mol^{-1}. These two changes are very large and significant. First of all, the reaction barrier increases under VSC as indicated by the increasingly positive enthalpy of activation. More importantly, the change in the sign of the entropy suggests a change in the nature of the transition state. This reaction typically proceeds through an associative reaction pathway whereby the initial step is fluorine attack on the silicon atom to form an intermediate with pentavalent coordination.[12] For such reaction mechanisms, $\Delta S^{\ddagger}$ is typically negative, and the activation barrier is low, as observed for the reaction outside the cavity. In contrast, a higher barrier ($|\Delta H^{\ddagger}|$) and a positive $\Delta S^{\ddagger}$ value are typical of a dissociative transition state, that is, the C–Si

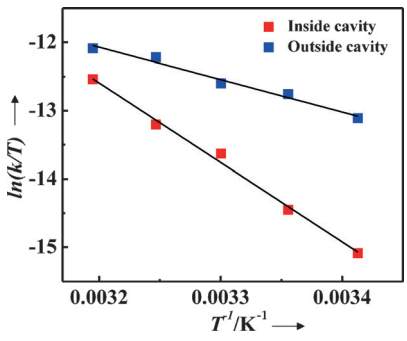

Figure 4. The reaction rate ([PTA] = 2.53 M, $\hbar\Omega_{VR}$ = 98 cm^{-1}) as a function of temperature (Eyring equation plot) for reactions inside the ON resonance cavity (red squares) and outside the cavity (blue squares).

bond starts breaking before the silicon center is attacked by the fluorine. This thermodynamic analysis, which is based on values extracted by transition-state theory, implies an adiabatic process. The possibility that non-adiabatic processes contribute to the reaction mechanism, and therefore to the extracted thermodynamics values, cannot be excluded. Indeed, the strong effect of 10% VSC Rabi splitting on the reaction pathway is a sure sign that the vibrational and electronic manifolds are strongly interacting. Furthermore, as we saw that the change in the reaction rate depends on the Rabi splitting, we expect that the thermodynamic parameters will vary accordingly.

This demonstration that VSC can significantly modify chemical landscapes opens many new possibilities for reaction control and shows that VSC provides a new approach for studying reaction mechanisms. As the molecules are randomly oriented and as coupling depends on the orientation of their transition dipole moments relative to the electromagnetic field in the cavity, not all molecules in the cavity are coupled at any given time (i.e., the molecules rotate much faster than the timescale of the overall reaction). Hence the observed changes under VSC are average values, making these findings even more remarkable. The dependence of the reaction rate on the collective Rabi splitting shows how the latter controls the reaction at the level of each molecule by changing their ground-state energy landscape. While we found that in our case, the reaction was slowed down, it is possible that depending on the chemical landscape, reaction rates can also be accelerated. When the reaction leads to multiple products, it is likely that the product ratios are modified under VSC, providing a way to optimize the yield of a given product. Site-selective chemical reactions are another possibility that should be explored. Finally, chemistry under VSC has the advantage that it works in the dark and at room temperature.

The coupling of molecular electronic transitions to the vacuum field has been more extensively studied[13–18] than VSC and has already shown many exciting results, such as enhanced conductivity[19] and non-radiative energy transfer,[20] lasing,[21] and condensation.[22] Together with VSC, it clearly opens many new possibilities for molecular and materials science that should be fully explored.

Experimental Section

All compounds were purchased from Sigma–Aldrich (analytical grade). All the spectroscopic data shown (except Figure 3a) correspond to the reactions carried out by mixing PTA (0.76 mmol, 150 μL) with TBAF (0.11 mmol, 28 mg) in methanol (3.7 mmol, 150 μL) and injecting about 2 μL of this mixture into the liquid sample cell unit. This particular concentration ([PTA] = 2.53 M) gave a high Rabi splitting and was devoid of any miscibility problems between PTA and TBAF solution at all temperatures under investigation. The concentration-dependent experiments were carried out by varying the PTA concentration from 0.87 M to 3.37 M at a TBAF concentration of 0.36 M ([MeOH] was varied to maintain [TBAF]). The flow cell, compatible with temperature-controlled measurements, was purchased from Specac. The Fabry–Perot cavity was obtained by sandwiching ZnSe windows, coated with a Au (10 nm) film and 100 nm of glass to ensure chemical insulation from the metal, with Mylar spacers (ca. 6 μm). The spectra of the cavity reactions were acquired with a standard FTIR spectrometer (Nicolet 6700) in transmission mode. The transmission was collected with a DTGS (deuterated triglycine sulfate) detector with 1 cm^{-1} resolution over 32 scans. The gas chromatograms were obtained by GC-MS analysis on a GC System 7820A (G4320) connected to an MSDblock 5977E (G7036A) using an Agilent high-resolution gas chromatograph. For GC-MS measurements, the reaction was followed spectroscopically for 20 min before the reaction mixture was immediately injected into the GC-MS column. At [PTA] = 3.37 M, roughly 2 μL of the sample were transferred to the GC-MS by washing (and diluting it) in 1.5 mL isopropanol.

Acknowledgements

We acknowledge support from the International Center for Frontier Research in Chemistry (icFRC, Strasbourg), the ANR Equipex Union (ANR-10-EQPX-52-01), the Labex NIE projects (ANR-11-LABX-0058 NIE), and CSC (ANR-10-LABX- 0026 CSC) and USIAS within the Investissement d'Avenir program ANR-10-IDEX-0002-02.

Keywords: IR spectroscopy · kinetics · strong coupling · thermodynamics · vibrations

How to cite: *Angew. Chem. Int. Ed.* **2016**, *55*, 11462–11466
Angew. Chem. **2016**, *128*, 11634–11638

[1] H. Frei, L. Fredin, G. C. Pimentel, *J. Chem. Phys.* **1981**, *74*, 397–411.
[2] H. Frei, G. C. Pimentel, *J. Chem. Phys.* **1983**, *78*, 3698–3712.
[3] J. A. Hutchison, T. Schwartz, C. Genet, E. Devaux, T. W. Ebbesen, *Angew. Chem. Int. Ed.* **2012**, *51*, 1592–1596; *Angew. Chem.* **2012**, *124*, 1624–1628.
[4] A. Shalabney, J. George, J. A. Hutchison, G. Pupillo, C. Genet, T. W. Ebbesen, arXiv: 1403.1050, **2014**; A. Shalabney, J. George, J. A. Hutchison, G. Pupillo, C. Genet, T. W. Ebbesen, *Nat. Commun.* **2015**, *6*, 5981.
[5] J. George, A. Shalabney, J. A. Hutchison, C. Genet, T. W. Ebbesen, *J. Phys. Chem. Lett.* **2015**, *6*, 1027–1031.
[6] A. Shalabney, J. George, H. Hiura, J. A. Hutchison, C. Genet, P. Hellwig, T. W. Ebbesen, *Angew. Chem. Int. Ed.* **2015**, *54*, 7971–7975; *Angew. Chem.* **2015**, *127*, 8082–8086.
[7] a) J. P. Long, B. S. Simpkins, *ACS Photonics* **2015**, *2*, 130–138; b) B. S. Simpkins, K. P. Fears, W. J. Dressick, B. T. Spann, A. D. Dunkelberger, J. C. Owrutsky, *ACS Photonics* **2015**, *2*, 1460–1467.
[8] J. del Pino, J. Feist, F. J. Garcia-Vidal, *New J. Phys.* **2015**, *17*, 053040.
[9] G. C. G. Waschewsky, P. W. Kash, T. L. Myers, D. C. Kitchen, L. J. Butler, *J. Chem. Soc. Faraday Trans.* **1994**, *90*, 1581–1598.
[10] P. V. James, P. K. Sudeep, C. H. Suresh, K. G. Thomas, *J. Phys. Chem. A* **2006**, *110*, 4329–4337.
[11] T. W. Ebbesen, submitted.
[12] J. Clayden, N. Greeves, S. Warren, P. Wothers, *Organic Chemistry*, 2nd ed., Oxford University Press, Oxford, **2012**.
[13] J. Galego, F. J. Garcia-Vidal, J. Feist, *Phys. Rev. X* **2015**, *5*, 041022.
[14] J. Feist, F. J. Garcia-Vidal, *Phys. Rev. Lett.* **2015**, *114*, 196402.
[15] P. Vasa, W. Wang, R. Pomraenke, M. Maiuri, C. Manzoni, G. Cerullo, C. Lienau, *Phys. Rev. Lett.* **2015**, *114*, 036802.
[16] Y. W. Hao, H. Y. Wang, Y. Jiang, Q. D. Chen, K. Ueno, W. Q. Wang, H. Misawa, H. B. Sun, *Angew. Chem. Int. Ed.* **2011**, *50*, 7824–7828; *Angew. Chem.* **2011**, *123*, 7970–7974.

[17] L. Shi, T. K. Hakala, H. T. Rekola, J. P. Martikainen, R. J. Moerland, P. Törmä, *Phys. Rev. Lett.* **2014**, *112*, 153002.
[18] J. Bellessa, C. Bonnand, J. C. Plenet, J. Mugnier, *Phys. Rev. Lett.* **2004**, *93*, 036404.
[19] E. Orgiu, J. George, J. A. Hutchison, E. Devaux, J. F. Dayen, B. Doudin, F. Stellacci, C. Genet, J. Schachenmayer, C. Genes, G. Pupillo, P. Samori, T. W. Ebbesen, *Nat. Mater.* **2015**, *14*, 1123 – 1129.
[20] X. Zhong, T. Chervy, S. Wang, J. George, A. Thomas, J. A. Hutchison, E. Devaux, C. Genet, T. W. Ebbesen, *Angew. Chem. Int. Ed.* **2016**, *55*, 6202 – 6206; *Angew. Chem.* **2016**, *128*, 6310 – 6314.
[21] S. Kéna Cohen, S. R. Forrest, *Nat. Photonics* **2010**, *4*, 371 – 375.
[22] J. D. Plumhof, T. Stöferle, L. Mai, U. Scherf, R. F. Mahrt, *Nat. Mater.* **2014**, *13*, 247 – 252.

Received: June 6, 2016
Published online: August 16, 2016

